

## Low-fidelity crashworthiness assessment of unconventional aircraft: Modelling of plastic bending

Anand, S.; Alderliesten, R.C.; Castro, Saullo G.P.

**DOI**

[10.2514/6.2024-0833](https://doi.org/10.2514/6.2024-0833)

**Publication date**

2024

**Document Version**

Final published version

**Published in**

Proceedings of the AIAA SCITECH 2024 Forum

**Citation (APA)**

Anand, S., Alderliesten, R. C., & Castro, S. G. P. (2024). Low-fidelity crashworthiness assessment of unconventional aircraft: Modelling of plastic bending. In *Proceedings of the AIAA SCITECH 2024 Forum* Article AIAA 2024-0833 (AIAA SciTech Forum and Exposition, 2024). American Institute of Aeronautics and Astronautics Inc. (AIAA). <https://doi.org/10.2514/6.2024-0833>

**Important note**

To cite this publication, please use the final published version (if applicable).  
Please check the document version above.

**Copyright**

Other than for strictly personal use, it is not permitted to download, forward or distribute the text or part of it, without the consent of the author(s) and/or copyright holder(s), unless the work is under an open content license such as Creative Commons.

**Takedown policy**

Please contact us and provide details if you believe this document breaches copyrights.  
We will remove access to the work immediately and investigate your claim.

# Low-fidelity crashworthiness assessment of unconventional aircraft: Modelling of plastic bending

Shreyas Anand\*, René Alderliesten<sup>†</sup> and Saullo G.P. Castro<sup>‡</sup>  
*Delft University of Technology, Delft, Zuid-Holland, 2628CD*

Carbon emissions from commercial aircraft are expected to reach more than twice as much as the current levels by 2050. Unconventional aircraft, such as the Flying-V, are projected to achieve more than 20% fuel savings when compared to conventional configurations. However, these unconventional aircraft configurations pose a unique set of design challenges, being one of them the crashworthiness of wing-fuselage structures, which have an oval-shaped cross section that leads to a significant reduction in space underneath the cabin floor. Evaluating the feasibility of a design early in the design phase is vital to avoid cost overruns and minimize the need for drastic design changes. For assessing crashworthiness early in the design phase, the development of low-fidelity models is an attractive as well as a viable option because these models offer both low computational cost and the capability to conduct parametric studies on the crash structure. To develop and implement such low-fidelity models, we propose to explore the analytical modeling of various energy-absorbing mechanisms, namely axial crushing, plastic bending, and joint failure. In the present study, we present the modelling of plastic bending for beam-like structural members. We also present an envisaged method applying user-defined elements to simulate plastic bending in structural members for cases where the location of plastic hinges cannot be predetermined.

## I. Nomenclature

$z_{max}$	=	Distance of outermost layer from neutral axis
$\epsilon_u$	=	Ultimate strain
$\rho$	=	Radius of curvature
$\epsilon(z)$	=	Strain distribution with respect to fiber distance from neutral axis
$\sigma(z)$	=	Stress distribution with respect to fiber distance from neutral axis
$A$	=	Cross sectional area
$M_{CS}$	=	Moment at a cross section
$dx$	=	Length of beam element
$d\theta$	=	Rotation of the beam element
$L_{RL}$	=	Length of rigid linkage

## II. Introduction

AVIATION is responsible for a big share of current carbon emissions, if left unchecked the carbon emissions from aircraft are expected to more than double by the year 2050 [1]. To prevent such a scenario, the International Air Transport Association (IATA) has defined a strategy to make the aviation industry carbon neutral by the end of year 2050 [2]. In their strategy, they attribute 13% reduction in emissions to more efficient aircraft design and new propulsion technologies [Fig. 1].

If unconventional aircraft become a reality, they will signify the next big leap in aircraft efficiency. Oosterom and Vos (2022) [3] predict a potential reduction of up to 22% in fuel burn for the Flying-V, when compared to the Airbus A350. However, unconventional aircraft cannot take to the skies if they are not at least equivalent in terms of crash

\*PhD Candidate, Aerospace Structures and Materials, s.anand@tudelft.nl

<sup>†</sup>Associate Professor, Aerospace Structures and Materials, r.c.alderliesten@tudelft.nl

<sup>‡</sup>Associate Professor, Aerospace Structures and Materials, s.g.p.castro@tudelft.nl

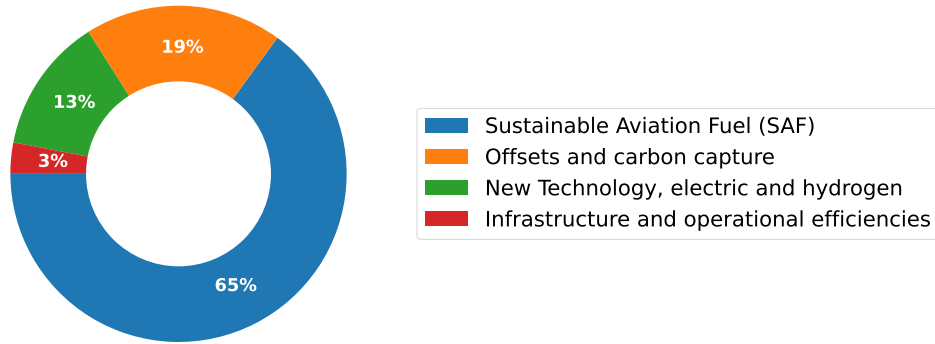


**Fig. 1 IATA strategy to achieve net zero carbon emissions by 2050 [2]**

safety, when compared to conventional aircraft. Achieving an equivalent amount of crash safety is difficult because crash structure design in the case of unconventional aircraft is significantly more challenging due to various factors:

- Reduced distance between the cabin floor and the ground: A smaller crushing distance means more deceleration to absorb the same amount of energy. Since the human body can only take a certain amount of deceleration without suffering serious injuries, it makes the design of crash structure more challenging.
- Absence of historical crash data: Conventional aircraft frequently use historical crash data to improve the design of crash structure. The crash structure of conventional aircraft has gradually developed into its current form, but for the case of unconventional aircraft such historical data is totally absent.
- Different crash scenarios: Due to their significantly different configuration, unconventional aircraft are subject to very different crash scenarios as compared to a conventional aircraft, meaning that current methods to show crashworthiness might not be enough.

These challenges demand approaches that can predict the crashworthiness of unconventional aircraft already at early stages of the design process. Since we want to iterate between various crash structural configurations and crash scenarios, it is important that the adopted models are fast enough to be compatible with the amount of iterations and parametric studies expected at early design phases. For the present study, we propose an analytical low-fidelity model to capture the plastic bending of beam-like elements, where the plastic hinge point is unknown.

### III. State of the art

Currently, the plastic bending of metallic structures can be simulated with great accuracy using numerical modeling techniques that require detailed models involving a high number of degrees of freedom. One of the commonly used methods for low-fidelity modeling of plastic bending consists of the spring-linkage model, which divides a beam section into multiple rigid linkages connected by torsional springs. Multiple authors have used this technique to model plastic bending for various materials and geometries. Lo et al. [4, 5] proposed using a spring-linkage model to study the forces acting on a section of the bonding wire and also demonstrated the modeling of a simple cantilever beam using a spring-linkage model with elastic-perfectly plastic assumption. In the set of equations proposed by Lo et al., the applied forces are treated as unknowns while the deformation, length of rigid linkages and the spring stiffness are treated as known parameters. Sousa et al. [6] used a variety of kinematic joints [Fig. 2] to simulate plastic hinges for their road vehicle crashworthiness model. In their work, Sousa et al. [6] applied finite element models of structural subsystems to get constitutive relationships for the kinematic joints.

More recently, a spring-linkage modeling approach was used by Tay et al. [7] to simulate plastic bending in aircraft frame sections. The authors propose representing a beam as a spring-linkage model with characteristic curves for each joint obtained using Finite Element Method (FEM). In their work, an "I"-shaped beam was used, with the proposed methodology achieving reasonable agreement between the Multi-Body (MB) model and Finite Element Analysis (FEA) model for the deceleration versus time curves, at various locations along the fuselage section. Moreover, Tay et al. [7] also showed good agreement with experimental results. Furthermore, the use of spring-linkage model is not only limited to metallic structures, and a similar methodology was used by Schatrow et al. [8] to simulate the crash of composite fuselage structures, utilizing joints whose stiffness is given by moment versus rotation curves to simulate the bending of

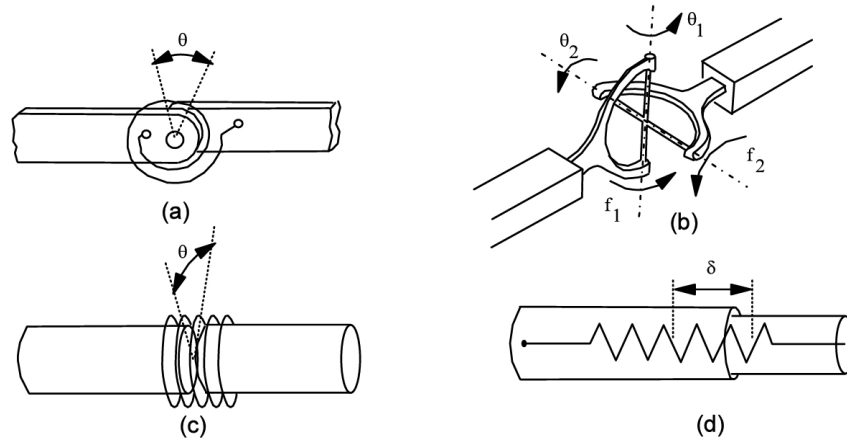


**Fig. 2 Kinematic joints used by Sousa et al. [6] for modeling plastic hinges under different loading conditions (a) One-axis bending (b) Two-axis bending (c) Torsion (d) Crushing**

composite frames. It is also important to note here that, in their case, the linkages were not rigid but instead modeled using finite elements. The authors also used their hybrid FE/Macro model to study different crash kinematics and obtain vertical accelerations that passengers will be subjected to during an impact.

From these results, it is evident that spring-linkage models give sufficiently accurate results when simulating crash impacts. However, two challenges need to be addressed before we can apply the spring-linkage model to study crashworthiness early in the design phase for unconventional aircraft:

- 1) For our application, obtaining the moment versus rotation curves for torsional springs through experimentation or FEM is not an option, as we want the ability to parameterize the model. Therefore, an analytical methodology to determine the moment versus rotation curve based on the geometrical and material parameters of the structural element is required.
- 2) It is important to note that the spring-linkage model relies on the positioning of springs at the locations where plastic hinges can be expected. Since unconventional aircraft have much less available crushing distance as compared to conventional aircraft, more complex crash structures will be required to maintain the same levels of deceleration for the passengers. This increase in the complexity of the structure means that it might not be possible to predetermine the location of plastic hinge points.

To address the first challenge, we propose an algorithm in section V.A which calculates the moment and corresponding rotation for a beam element of length  $dx$ . The second challenge can be addressed by discretizing the beam into greater number of springs and linkages, ensuring that there are enough spring elements to model a plastic hinge at any point on the beam. However, discretizing the beam assuming that a plastic hinge can occur at any point on the beam would increase the degrees of freedom of the spring-linkage model making the model more resource intensive and is therefore not a well-suited option for studying crashworthiness early in the design phase.

It is interesting to note that the second challenge of predicting the location of plastic hinges is similar to the numerical modeling of cracks and discontinuities, where cracks can only propagate along the element boundaries. For the modeling of cracks, various ideas have been proposed in the literature, such as the finite element-based approach for automatic tracking of the crack propagation which was proposed by Shephard et al. [9] as early as 1985. Their approach takes into account the crack propagation and re-meshes the geometry for an accurate representation of reality. Similar adaptive mesh update techniques have been proposed in the works of various other authors [10–12]. Since remeshing after each step is not efficient in terms of computational cost, other methods that avoid remeshing have also been proposed in the literature, and one such method is the Phantom Node Method (PNM) [13–15]. In the PNM, if an element is divided by a crack, extra nodes are used to superpose two elements at the location of the original element and computations are only performed in active parts of the new elements.

Although the examples for crack growth deal with finite element methods, it is possible to take a cue from these approaches to create a model with user-defined elements that can adapt to the changes in constraints and, therefore, the

location of the plastic hinges. An envisaged method with such user-defined elements is given in section V.B.

#### IV. Materials and Methods

To determine the accuracy of spring-linkage model, deflection and energy absorption results obtained using spring-linkage model were compared against results obtained using Finite Element Method (FEM). FEM simulations were performed in Abaqus [16] using C3D8R elements for cantilever and simply supported beams, with the force being applied as a ramp input. Dimensions for rectangular and I-shaped cross-sections are given in Figure 3. The material used for beam elements was aluminum alloy AA6060-T4. Simulations were conducted for a cantilever beam of 1000 mm length and a simply supported beam of 2000mm length. The spring-linkage model and the algorithm to obtain moment vs rotation curves for torsional spring elements were both implemented in Python.

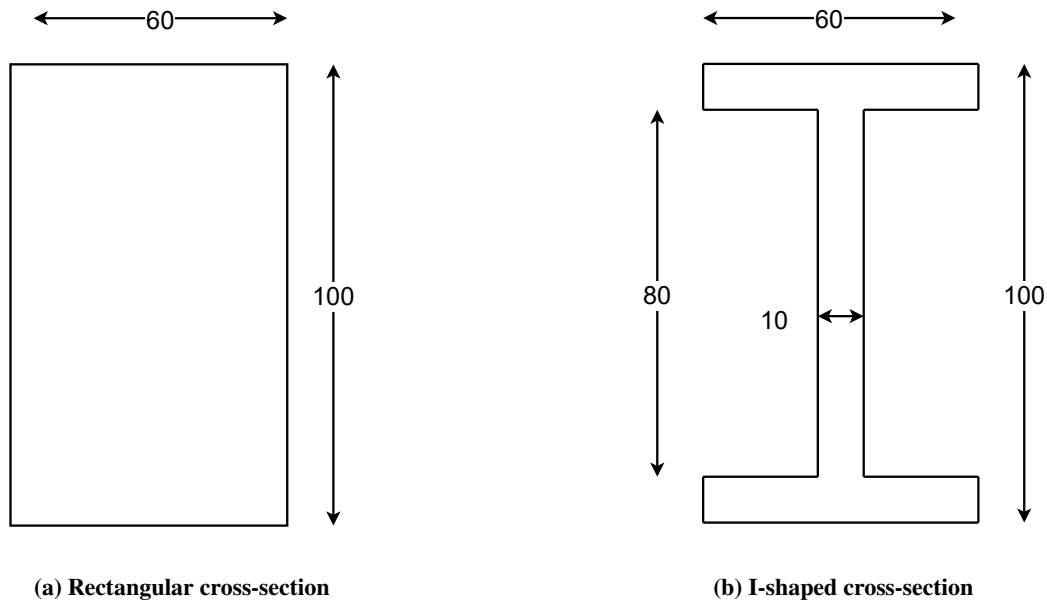


Fig. 3 Dimensions for rectangular and I-shaped cross-sections

For the spring-linkage model, the moment vs rotation curves for each spring element is obtained using the algorithm presented in section V.A. Subsequently, the applied moment at each spring was computed and the rotation at each spring was determined using a lookup function. Using the obtained rotation values, vertical and horizontal displacements were then calculated for each rigid linkage. The energy absorption for each spring in the spring-linkage model was computed using the area under moment versus rotation curve. Total energy absorption of the model was then determined by summing the contributions from all individual springs.

#### V. Modelling of plastic hinge

Based on the state of the art discussed in the previous section, this section discusses in further detail the two challenges in application of the spring-linkage model to plastic bending. The first subsection (section V.A) presents an algorithm for obtaining moment versus rotation curves for torsional springs using geometrical and material properties of the beam element. The second subsection (section V.B) discusses in further detail an approach to account for new plastic hinge locations during bending of a beam section.

##### A. Algorithm to analytically obtain moment versus rotation curves for symmetric cross-sections

To analytically obtain the moment versus rotation curve for the beam section we begin from the relation between radius of curvature and fiber strain, the following steps are proposed:

- 1) Calculate the radius of curvature ( $\rho_u$ ) for which the outermost layer reaches ultimate strain ( $\varepsilon_u$ ):

$$\rho_u = \frac{z_{max}}{\varepsilon_u} \quad (1)$$

Where  $z_{max}$  is the distance of outermost layer from the neutral axis.

- 2) Iterate between the obtained radius of curvature ( $\rho_u$ ) and infinity ( $\rho \approx 10^6$ , signifying 0 curvature) to obtain corresponding values of strain at the outermost layer. We assume a linear strain distribution with respect to layer distance from the neutral axis,  $\varepsilon(z)$ .
- 3) Discretizing the beam element along the height into "n" elements, the stress distribution is then obtained using the stress-strain relationship. For each value of strain ( $\varepsilon$ ), the corresponding stress ( $\sigma$ ) value is obtained by using a lookup function.
- 4) Once the stress distribution is known, the moment corresponding to the given radius of curvature and strain distribution can then be calculated using equation 2.

$$M_{CS} = \sum_{i=1}^n (\sigma_i \cdot z_i \cdot A_i) \quad (2)$$

- 5) For a small element of length dx, we can obtain the rotation ( $d\theta$ ) using equation 3:

$$dx = d\theta \cdot \rho \quad (3)$$

- 6) As the moment and rotation corresponding to the radius of curvature are now known, we can plot the moment versus rotation curve for a beam element of length dx. The length dx must be small enough to ignore the variation in moment along the beam axis.
- 7) To reduce the number of computations further, we can calculate moment versus rotation curves for beam elements of greater length by taking into account the expected moment distribution and adding the rotational contribution of each small element of length dx.

Figure 4 illustrates the procedure in the form of a flowchart. The obtained moment versus rotation curves are then provided as an input for spring stiffness in the spring-linkage model. It is important to note here that this algorithm needs to be repeated for beam elements of different lengths. However, the run time of the algorithm is small enough ( $\approx 2.8s$  using a python script) to allow for such computations during the simulation. Alternatively, a database of moment versus rotation curves can be generated as part of pre-processing for various possible rigid element lengths before proceeding with bending calculations using the spring-linkage model. The results obtained using this algorithm are presented in section VI.

## B. Envisaged method with user-defined elements

The spring-linkage model has a significant deficiency, as it requires the user to place spring elements in the locations where plastic hinges can be expected in order to obtain accurate results. For complex crash structures, predicting the location of plastic hinges can be difficult as new constraints can be introduced during the collapse of the crash structure. One can overcome this problem by increasing the number of joints in an arbitrary manner, but that would directly reduce the computational efficiency of the model. Taking a cue from crack growth methods, we propose to take a user element based approach which accounts for external contacts and stresses in the beam structure to predict the location of plastic hinges. Once the position of the plastic hinge is known, the geometry can be remeshed with a joint element placed at the predicted location of the plastic hinge.

To introduce new joint elements at possible locations during a bending simulation, we first need an algorithm which can predict the location of external forces/contacts and secondly, a beam formulation which can easily take these constraints into account. Both of these requirements can be satisfied using a Lagrangian formulation for the model because Lagrangian formulation can be used to track the motion of individual beam elements and also because external constraints can be easily incorporated using Lagrangian multipliers.

A crash simulation can then be performed using the spring-linkage model as the basis but replacing the rigid linkages with user elements that are activated when external forces/ contacts are encountered. This activation can be done using an algorithm that predicts the possible intersection of elements based on their motion. Once a possible location for the

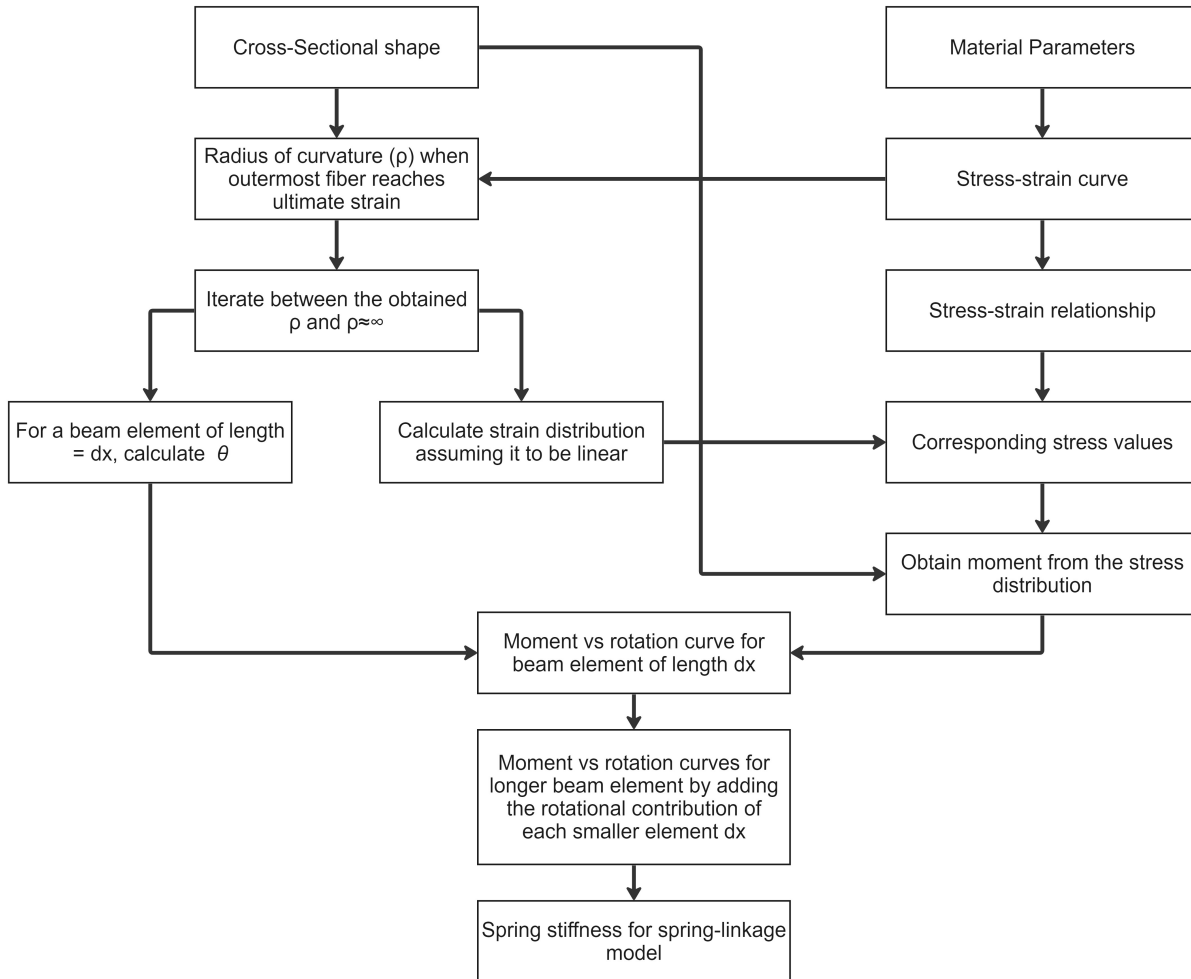


**Fig. 4 Flowchart to obtain characteristic curves for the spring-linkage model**

plastic hinge has been identified, a new joint is added and the moment versus rotation between the sub elements can be computed using the algorithm presented in section V.A.

This envisaged approach is still a work in progress. However, to demonstrate the possibility of using such a methodology for modelling of plastic bending, we present two relevant cases of a rectangular beam with an intermediate rigid surface as a part of this paper. The first case consists of a rectangular beam discretized into equally spaced elements in such a manner that there is a joint present at the intermediate rigid surface location (location of plastic hinge) and a second case where a new joint element is introduced at the intermediate rigid surface location. Results for both of these cases are presented in section VI.

## VI. Results

This section presents the comparison of results obtained using spring-linkage model and results obtained using FEM for various bending scenarios. These results are further divided into three sub-sections, the first sub-section (VI.A) presents results for bending of cantilever and simply supported beams to test the accuracy of spring-linkage model with analytically derived moment versus rotation curves. The second sub-section (VI.B) studies the influence of rigid linkage length on the deflection and energy absorption predictions. Finally, the third sub-section (VI.C) presents the results obtained for bending simulations with an intermediate rigid surface to test the possibility of using spring-linkage model for predicting deflection and energy absorption in cases where the location of plastic hinge cannot be predetermined.

### A. Cantilever and Simply supported beams

This section presents the results obtained for cantilever and simply supported beams using spring-linkage model with analytically obtained moment versus rotation curves. Obtained deflection and energy absorption are compared with results obtained using FEM. Following test cases were studied:

- 1) **Test case 1:** Cantilever beam with a rectangular cross-section (Figures 5a and 5b)
- 2) **Test case 2:** Simply-supported beam with a rectangular cross-section (Figure 5c and 5d)
- 3) **Test case 3:** Cantilever beam with an I-shaped cross-section (Figures 5e and 5f)
- 4) **Test case 4:** Simply-supported beam with an I-shaped cross-section (Figures 5g and 5h)

S.No.	Cross-section	Configuration	Max deflection error (%)	Energy absorption error (%)
1	Rectangular	Cantilever	-3.59	1.61
2	Rectangular	Simply supported	-1.58	4.47
3	I-shaped	Cantilever	1.45	5.85
4	I-shaped	Simply supported	-1.25	-2.10

**Table 1 Error in max deflection and energy absorption for cantilever and simply supported beams**

Results obtained for all the cases and the corresponding errors are given in Table 1. From the obtained results it is evident that the spring-linkage model with analytically obtained moment versus rotation curves can adequately represent the bending of beams, with an error percentage of less than 6% for max deflection and energy absorption for the studied cases.

### B. Influence of rigid linkage length ( $L_{RL}$ )

This section presents the results obtained for different rigid linkage lengths ( $L_{RL}$ ). For a cantilever beam of 1000 mm length, the rigid linkage lengths ( $L_{RL}$ ) used were:  $L_{RL} = [25, 50, 100, 200]$ . As expected the accuracy of the model increased with a decrease in rigid linkage length  $L_{RL}$ , for example, the error in energy absorption was found to be 13.72% for  $L_{RL} = 200$  and 1.18% for  $L_{RL} = 25$ . The results are presented in Table 2 and Figure 6.

S.No.	Rigid linkage length ( $L_{RL}$ )	Tip deflection error (%)	Energy absorption error (%)
1	25	-1.02	1.18
2	50	-3.59	1.61
3	100	-5.59	5.48
4	200	-8.68	13.72

**Table 2 Error in tip deflection and energy absorption for different values of rigid linkage lengths ( $L_{RL}$ ) in case of a cantilever beam**

### C. Bending simulations with intermediate rigid surface

Two cases were studied for bending simulations with an intermediate rigid surface, the first case consists of a rectangular beam discretized with equally spaced torsional springs such that there is a joint present at the location of plastic hinge and a second case where a new joint element is introduced at the location of plastic hinge. The results for these simulations are presented in Figure 7. For the first case, error in deflection was -0.18% and error in energy absorption was -1.49%. And for the second case, error in deflection was 1.47% and error in energy absorption was 5.92%.

## VII. Conclusions

The results obtained using spring-linkage model with analytically obtained moment versus rotation curves are promising, with the error in both deflection and energy absorption decreasing below 1.2% with a rigid linkage length ( $L_{RL}$ ) of 25mm. For the case where a new joint element is introduced to account for an intermediate rigid surface, the



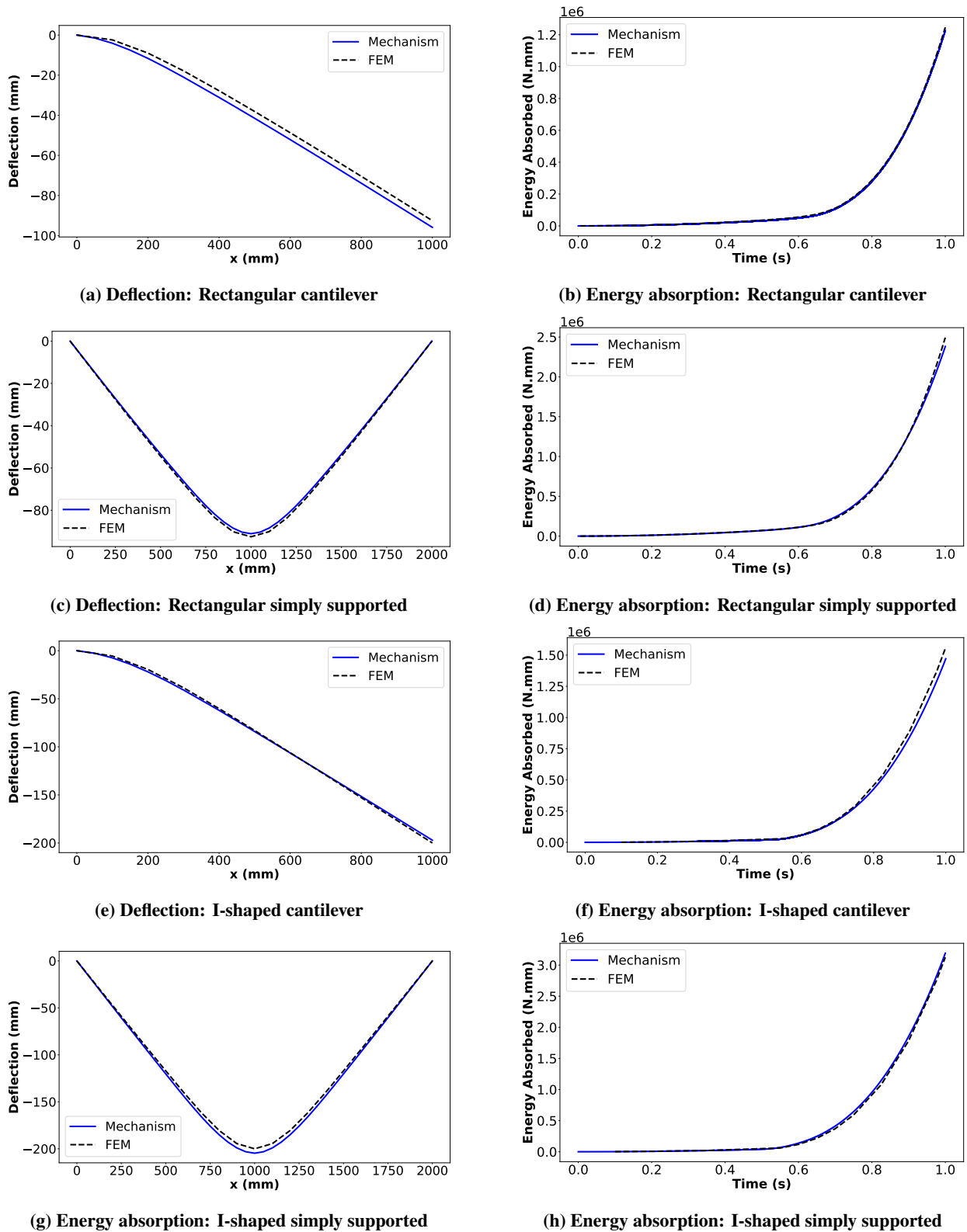
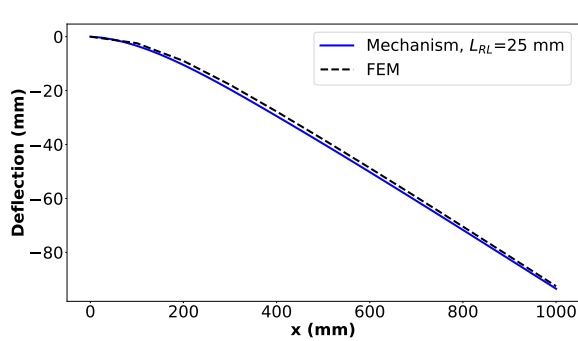
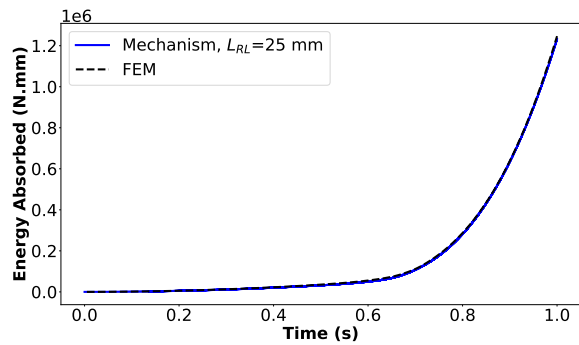


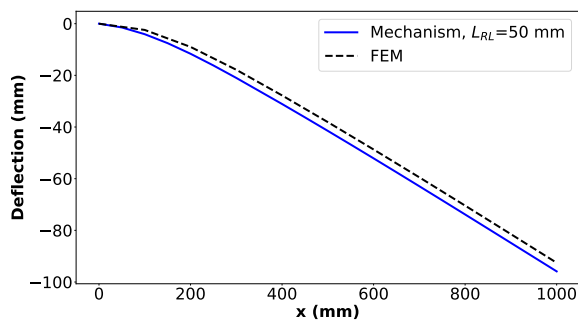
**Fig. 5 Comparison of spring-linkage model deflection and energy absorption against FEM for cantilever and simply supported beams with rectangular and I-shaped cross-sections**



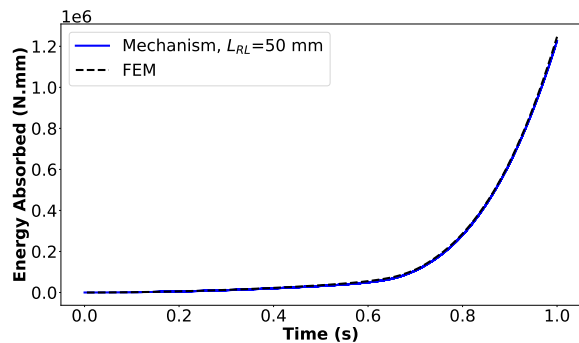
(a) Deflection:  $L_{RL} = 25$  mm



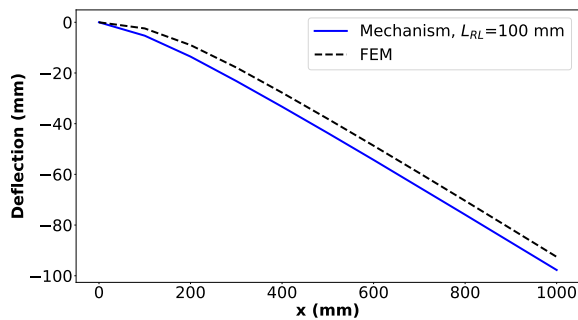
(b) Energy absorption:  $L_{RL} = 25$  mm



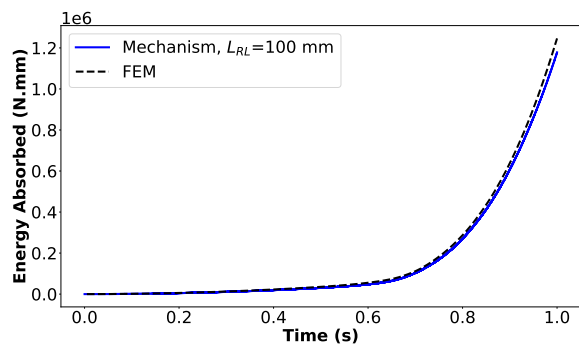
(c) Deflection:  $L_{RL} = 50$  mm



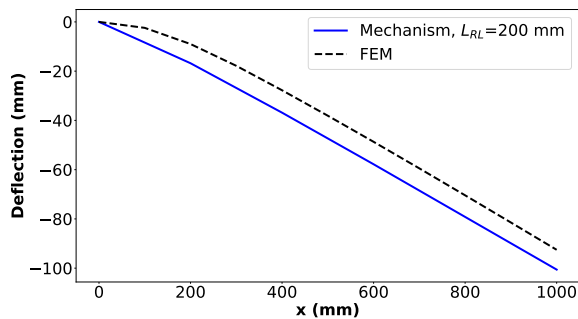
(d) Energy absorption:  $L_{RL} = 50$  mm



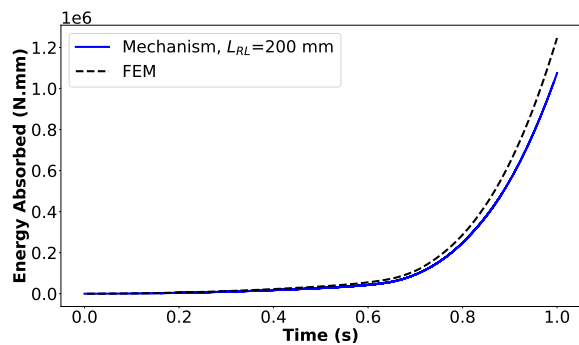
(e) Deflection:  $L_{RL} = 100$  mm



(f) Energy absorption:  $L_{RL} = 100$  mm

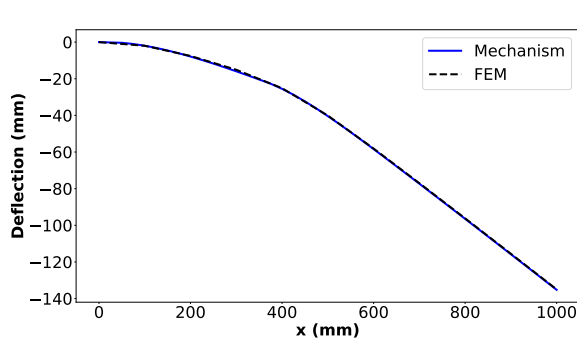


(g) Deflection:  $L_{RL} = 200$  mm

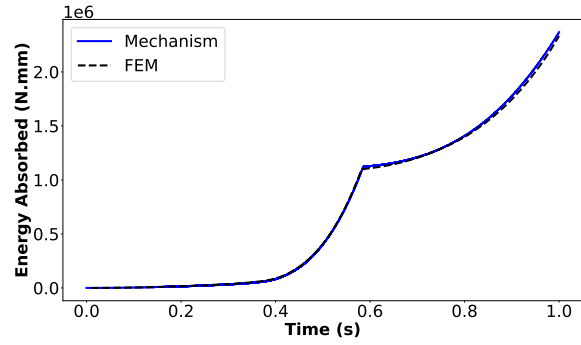


(h) Energy absorption:  $L_{RL} = 200$  mm

**Fig. 6 Comparison of spring-linkage model deflection and energy absorption against FEM for different values of rigid linkage lengths ( $L_{RL}$ ) in case of a cantilever beam**

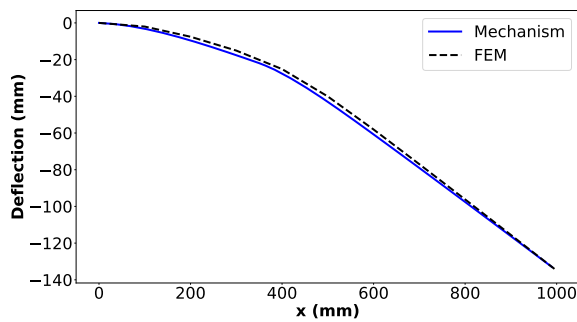


(a) Deflection

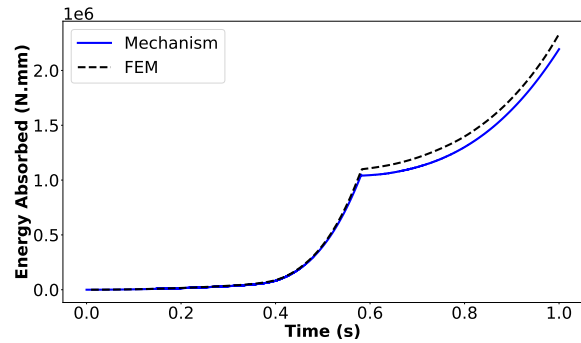


(b) Energy absorption

(c) Comparison against FEM for spring-linkage model with equally spaced torsional springs



(d) Deflection



(e) Energy absorption

(f) Comparison against FEM for spring-linkage model with torsional spring inserted at the location of plastic hinge

**Fig. 7 Comparison of spring-linkage model with FEM for cantilever beam with intermediate rigid surface**

error in maximum deflection was 1.47% and the error in energy absorption was 5.92%, reinforcing the applicability of spring-linkage model for cases where the location of plastic hinges cannot be predetermined. However, spring-linkage model should be employed with care as the obtained results were observed to be very sensitive to length of the rigid linkages (section VI.B). We plan to implement the spring-linkage model using Lagrangian formulation to easily account for new constraints, such an approach will enable computationally efficient simulation of bending for fuselage structures undergoing impact, even for more complex unconventional structures where the location of plastic hinges cannot be predetermined and will consequently also enable parametric studies of different crash structures for unconventional aircraft configurations. Further investigation is also required to test the applicability of spring-linkage model for simulating plastic bending of curved beams.

### Acknowledgments

The authors wish to express their sincere gratitude to TU Delft and the Smart Flying-V project supported by the faculty of aerospace engineering, for providing all the resources without which successful completion of this work would not have been possible.

### References

- [1] *Waypoint 2050*, 2<sup>nd</sup> ed., Air Transport Action Group (ATAG), 2021.
- [2] "Resolution on the industry's commitment to reach net zero carbon emissions by 2050," 2021. URL <https://www.iata.org/en/pressroom/pressroom-archive/2021-releases/2021-10-04-03/>.

- [3] Oosterom, W., and Vos, R., “Conceptual Design of a Flying-V Aircraft Family,” *AIAA AVIATION 2022 Forum*, American Institute of Aeronautics and Astronautics, 2022. <https://doi.org/10.2514/6.2022-3200>, URL <https://doi.org/10.2514/6.2022-3200>.
- [4] Lo, Y.-L., Ho, T.-L., Chen, J.-L., Lee, R.-S., and Chen, T.-C., “Linkage-spring model in analyzing wirebonding loops,” *IEEE Transactions on Components and Packaging Technologies*, Vol. 24, No. 3, 2001, pp. 450–456. <https://doi.org/10.1109/6144.946493>.
- [5] Lo, Y.-L., Chen, T.-C., and Ho, T.-L., “Design in triangle-profiles and T-profiles of a wirebond using a linkage-spring model,” *IEEE Transactions on Components and Packaging Technologies*, Vol. 24, No. 3, 2001, pp. 457–467. <https://doi.org/10.1109/6144.946494>.
- [6] Sousa, L., Veríssimo, P., and Ambrósio, J., “Development of generic multibody road vehicle models for crashworthiness,” *Multibody System Dynamics*, Vol. 19, 2008, pp. 133–158. <https://doi.org/10.1007/s11044-007-9093-z>.
- [7] Tay, Y. Y., Flores, P., and Lankarani, H., “Crashworthiness analysis of an aircraft fuselage section with an auxiliary fuel tank using a hybrid multibody/plastic hinge approach,” *International Journal of Crashworthiness*, Vol. 25, 2019, pp. 1–11. <https://doi.org/10.1080/13588265.2018.1524547>.
- [8] Schatrow, P., and Waimer, M., “Crash concept for composite transport aircraft using mainly tensile and compressive absorption mechanisms,” *CEAS Aeronautical Journal*, Vol. 7, 2016. <https://doi.org/10.1007/s13272-016-0203-6>.
- [9] Shephard, M., Weidner, T., Nabil, B., and Burd, G., “Automatic crack propagation tracking,” *Computers Structures*, Vol. 20, 1985. [https://doi.org/10.1016/0045-7949\(85\)90070-7](https://doi.org/10.1016/0045-7949(85)90070-7).
- [10] Askes, H., and Sluys, L. J., “Remeshing strategies for adaptive ALE analysis of strain localisation,” *European Journal of Mechanics - A/Solids*, Vol. 19, No. 3, 2000, pp. 447–467. [https://doi.org/10.1016/s0997-7538\(00\)00176-5](https://doi.org/10.1016/s0997-7538(00)00176-5), URL [https://doi.org/10.1016/s0997-7538\(00\)00176-5](https://doi.org/10.1016/s0997-7538(00)00176-5).
- [11] Swenson, D., and Ingraffea, A. R., “Modeling mixed-mode dynamic crack propagation using finite elements: Theory and applications,” *Computational Mechanics*, Vol. 3, 1988, pp. 381–397.
- [12] Koenke, C., Harte, R., Krätzig, W., and Rosenstein, O., “On adaptive remeshing techniques for crack simulation problems,” *Engineering Computations*, Vol. 15, No. 1, 1998, pp. 74–88. <https://doi.org/10.1108/02644409810200695>, URL <https://doi.org/10.1108/02644409810200695>.
- [13] Areias, P. M., Song, J., and Belytschko, T., “Analysis of fracture in thin shells by overlapping paired elements,” *Computer Methods in Applied Mechanics and Engineering*, Vol. 195, No. 41-43, 2006, pp. 5343–5360. <https://doi.org/10.1016/j.cma.2005.10.024>, URL <https://doi.org/10.1016/j.cma.2005.10.024>.
- [14] Song, J.-H., Areias, P. M. A., and Belytschko, T., “A method for dynamic crack and shear band propagation with phantom nodes,” *International Journal for Numerical Methods in Engineering*, Vol. 67, No. 6, 2006, pp. 868–893. <https://doi.org/10.1002/nme.1652>, URL <https://doi.org/10.1002/nme.1652>.
- [15] Meer, F. P., and Sluys, L. J., “A phantom node formulation with mixed mode cohesive law for splitting in laminates,” *International Journal of Fracture*, Vol. 158, No. 2, 2009, pp. 107–124. <https://doi.org/10.1007/s10704-009-9344-5>, URL <https://doi.org/10.1007/s10704-009-9344-5>.
- [16] “Abaqus/CAE User’s Guide,” *SIMULIA User Assistance 2021*, ??? URL [https://help.3ds.com/2021/English/DSSIMULIA\\_Established/SIMACAECAERefMap/simacae-c-ov.htm?contextscope=all&id=7d6038c876dd40b984c8f7cd798ba0b8](https://help.3ds.com/2021/English/DSSIMULIA_Established/SIMACAECAERefMap/simacae-c-ov.htm?contextscope=all&id=7d6038c876dd40b984c8f7cd798ba0b8).